International Journal of Nanomedicine

Dovepress
open access to scientific and medical research

Open Access Full Text Article

ORIGINAL RESEARCH

Modified magnetic nanoparticles by PEG-400-immobilized Ag nanoparticles (Fe_3O_4@PEG–Ag) as a core/shell nanocomposite and evaluation of its antimicrobial activity

This article was published in the following Dove Press journal:
International Journal of Nanomedicine

Kamiar Zomorodian[1,2]
Hamed Veisi[3]
Seyed Mahmoud Mousavi[4]
Mahmoud Sadeghi Ataabadi[5]
Somayeh Yazdanpanah[1,2]
Jafar Bagheri[1]
Ali Parvizi Mehr[1]
Saba Hemmati[3]
Hojat Veisi[3]

[1]Department of Medical Mycology, Basic Sciences in Infectious Diseases Research Center, School of Medicine, Shiraz University of Medical Sciences, Shiraz, Iran; [2]Department of Medical Mycology and Parasitology, School of Medicine, Shiraz University of Medical Sciences, Shiraz, Iran; [3]Department of Chemistry, Payame Noor University, Tehran, Iran; [4]Department of Medical Parasitology, Shiraz University of Medical Sciences, Shiraz, Iran; [5]Department of Reproductive Biology, School of Advanced Medical Sciences and Technologies, Shiraz University of Medical Sciences, Shiraz, Iran

Background: Noble metal nanoparticles, due to their good physicochemical properties, have been exploited in biological applications. Among these metals, nanosilver has attracted great attention because of its optical properties and broad-spectrum antimicrobial activities with no drug tolerance.

Purpose: The present study has attempted to conduct chemical synthesis of Fe_3O_4@PEG-Ag core/shell nanocomposites in aqueous solutions through co-precipitation of Fe^{3+} and Fe^{2+} ions, encapsulating the iron oxide core by poly (ethylene-glycol) (PEG) improve its hydrophilicity and biocompatibility, and immobilizing silver ions by application of $NaBH_4$ as a reducing agent.

Patients and methods: The synthesized structures were characterized by Fourier-transform infrared (FT-IR), field emission scanning electron microscopy, energy-dispersive X-ray spectrum, wavelength-dispersive X-ray, vibrating sample magnetometer, inductively coupled plasma-mass spectrometry and transmission electron microscopy methods. Antimicrobial activity of the nanostructures against *Staphylococcus aureus*, *Escherichia coli* and *Candida albicans* was evaluated by broth microdilution based on the methods suggested by Clinical Laboratory Standard Institute. Furthermore, the nanocomposite was tested for possible anti-parasitic effects against *Leishmania major* promastigotes by MTT assay. Also, its impacts on bacterial cell morphology were defined using atomic force microscopy. Moreover, toxicity of the nanostructure related to animal cell line was determined based on MTT assay.

Results: In general, the synthesized core/shell nanostructure can demonstrate noticeable activity against the evaluated representative microorganisms while its toxicity against animal cell line is not considerable.

Conclusion: This nanostructure can be applied as a smart drug delivery system with the help of an external magnetic field or it can be used as a powerful antibiotic agent along with other antibiotics that can form a shell on its structure.

Keywords: Poly-ethylene-glycol, nanocomposite, AgNPs, antimicrobial properties

Introduction

In the past 2 decades, functional nanomaterials have attracted great attention for their unique properties based on their size, shape and compositions.[1,2] Emergence of resistance against routine antibiotics has increased dramatically during this period. Some examples include nosocomial infections caused by methicillin-resistant *Staphylococcus aureus* (MRSA), azole-resistant *Candida* species and third-generation cephalosporin-resistant (TGCsR) *Escherichia coli*, which have ended up with high mortality and morbidity in patients.[3,4] Another crisis is associated with resistance to antiparasitic drugs, which is more critical in developing countries. Thereby, increased occurrence

Correspondence: Hojat Veisi
Department of Chemistry, Payame Noor University (PNU), P.O Box 19395-4697, Mini-city, Nakhl Street, Tehran, Iran
Tel +98 2332 0000
Fax +98 2244 1511
Email hojatveisi@yahoo.com

submit your manuscript | www.dovepress.com
Dovepress
http://dx.doi.org/10.2147/IJN.S161002

of resistance to Glucantime (meglumine antimoniate) has been reported by several researches.[5,6]

Consequently, some new antimicrobial agents with low cost, broad applicability, eco-friendliness, long lifetime and reusability features should be developed. An option to overcome antibiotic resistance is application of novel synthetic nanostructures with antimicrobial capabilities.[7–13] The nanostructure can be a metallic nanoparticle (NP). Since noble metal NPs possess good physicochemical properties, they have been used in biological applications. Among noble metals, silver has gained more interest due to its specific optical properties and diverted antimicrobial activities; however, it poses no drug tolerance.[14–24] Antimicrobial function of silver is effective in a way that it is safe for animal cells but very toxic for microorganisms (from fungi to viruses), eg, HIV, *E. coli* and *Staphylococcus aureus*. Nanosilver particles have high surface-to-volume ratio, small size and high dispersion potency, which facilitate their interactions with microbial surfaces. Thereby, they can be easily adhered to cell walls of different microorganisms to destroy and kill their cells by altering the permeability of cell membrane and disrupting the function of respiration system of pathogen cells. In addition, the genomic substance of cell containing nitrogen, oxygen and sulfur combines with Ag ions that leads to interception of DNA replication.[7,25–27]

On the other hand, much attention has been devoted to superparamagnetic magnetite (Fe_3O_4) nano-ferro particles as a result of their high magnetic saturation, low toxicity and facile surface modification using polymers, such as dextran,[28] poly(ethylene glycol) (PEG)[29] and polyvinylpyrrolidone (PVP).[25,26,30] A process requires for the solubility and bioavailability of metals used in NPs.[23] Specifically, PEG can demonstrate noticeable biocompatibility, biodegradability, blood circulation times and hydrophilicity.

Among the pathogen agents, *E. coli*, a Gram-negative bacteria; *S. aureus*, a Gram-positive bacteria; and also *Candida albicans*, a dimorphic yeast, are well-known factors reported as agents of nosocomial infections.[31] For this reason, the antimicrobial activity of synthesized NPs in various studies against these pathogen organisms has been considered. NPs of cadmium selenide,[32] zinc oxide-doped TiO_2,[33] binary metal oxide nanocomposites using cerium and cadmium[34] are studies that have exhibited antimicrobial effects of mentioned NPs. Furthermore, NPs have been made using plant extracts, which also have inhibitory effects on the growth of pathogens.[35,36]

Therefore, with respect to the earlier discussions, this study attempts to synthesize and characterize inorganic–organic hybrids (Fe_3O_4@PEG–Ag) as antimicrobial agents. These agents are expected as promising therapeutics due to their significant chemical stability, negligible toxicity, great hydrophilicity, heat resistance and long life.

Experimental

Materials

Chemicals were purchased from EMD Millipore (Billerica, MA, USA). The reagents and solvents were obtained from Sigma-Aldrich Co. (St Louis, MO, USA) and EMD Millipore and used without further purification.

Preparation of magnetic Fe_3O_4 nanoparticles (MNPs)

Fe^{2+} and Fe^{3+} ions with a molar ratio of 2:1 were chemically coprecipitated to prepare naked Fe_3O_4 NPs. Typically, $FeCl_2{\cdot}4H_2O$ (2.147 g, 0.0108 mol) and $FeCl_3{\cdot}6H_2O$ (5.838 g, 0.0216 mol) were dissolved in 100 mL of deionized water and vigorously stirred (500 rpm) at 85°C under nitrogen atmosphere. Then, 10 mL (one portion) of 25% NH_4OH was quickly added to the reaction mixture (Fe^{2+}/Fe^{3+} salt solution), while a black precipitate of MNPs was immediately formed. After another 25 min, the mixture was cooled to room temperature. Consequently, the ultrafine magnetic particles treated by magnetic separation were washed with deionized water several times.

Preparation of Fe_3O_4@PEG400

In all, 1 g of Fe_3O_4 NPs was dispersed in 200 mL of water and sonicated for 20 min. Then, 3 g of PEG400 dissolved in 10 mL of water was added to the solution and sonicated for 10 min again. Using an external magnet, the suspended substance yielded after mechanical agitation at 25°C for 24 h was separated to be washed with water and ethanol. After synthesizing PEG400-functionalized Fe_3O_4 (Fe_3O_4@PEG400), the NPs were dried at 50°C for 12 h.

Preparation of Fe_3O_4@PEG400/Ag

Fe_3O_4@PEG400 (200 mg) was dispersed in water (50 mL) and sonicated for 20 min. Subsequently, 20 mL of 10^{-2} M $AgNO_3$ solution was added to the reaction mixture and stirred for 2 h. Then, freshly prepared aqueous $NaBH_4$ solution (5×10^{-2} M, 25 mL) was added at one portion and stirred for 30 min at room temperature. Finally, the as-prepared nanocomposite was separated by an application of external magnetic field and washed several times by deionized water. The Ag loading of the prepared nanocomposite was measured to be 0.12 mmol/g by ICP.

Determination of biological activities of the microorganisms

The antimicrobial activity of Fe_3O_4@PEG–Ag was evaluated against four standard microorganism strains, including

C. albicans (ATCC 10261), *S. aureus* (ATCC 2592), *E. coli* (ATCC 25922) and isolated *Leishmania major* promastigotes (MRHO/IR/75/ER).

Antibacterial and antifungal activities

Minimum inhibitory concentration (MIC) values were explored through the broth microdilution method proposed by the Clinical Laboratory Standard Institute (CLSI) with some modifications.[37] Briefly, the antifungal activity was determined by serial dilution of the NP (0.5–512 µg/mL) in 96-well microtiter plates using the Roswell Park Memorial Institute (RPMI)-1640 medium (Sigma-Aldrich Co.), which was buffered with 3-(N-morpholino)propanesulfonic acid (Sigma-Aldrich Co.). To investigate the antibacterial activity of the NP, it was diluted serially (0.5–256 µL/mL) in a Müller-Hinton medium (EMD Millipore). To target yeasts and bacteria, three colonies of each microorganism were suspended in 5 mL of sterile 0.85% NaCl to give the stock suspensions, and inoculums' turbidity was adjusted on 0.5 McFarland standard at a wavelength of 630 nm. This preparation method provided stock suspensions of $1–5 \times 10^6$ cells/mL and $1–1.5 \times 10^8$ cells/mL for yeasts and bacteria, respectively. The working suspension was made by diluting the stock suspension with RPMI (1/1,000) or Müller-Hinton broth (1/100) solutions for yeasts and bacteria, respectively. In all, 0.1 mL of the working inoculum was injected to each well of the microtiter plates, and the plates were incubated at 32°C for 24–48 h for fungi or at 37°C for 24 h for bacteria in a humid atmosphere. A total of 200 µL of uninoculated medium was considered as a sterility blank control. Furthermore, growth controls, ie, media containing inoculums and no NP, were also evaluated. Microorganism growth in each well was examined versus the corresponding well of growth control. MICs were indicated visually to be the lowest concentration of NPs that can provide ≥95% reduction in microorganism growth as compared with the growth control wells.[23] Each experiment was repeated three times.

Moreover, the media of the yeast containing plate wells that exhibited no visible yeast growth were further cultured on Sabouraud dextrose agar (EMD Millipore) to determine the minimum fungicidal concentration (MFC). In addition, the media of bacteria consisting of wells with no apparent bacteria growth were cultured on Müller-Hinton agar (EMD Millipore) to recognize the minimum bactericidal concentration (MBC). MFCs and MBCs were identified as the lowest concentrations of microorganism producing no more than four colonies, which refers to a 98% microorganism mortality in the initial inoculums. Concentrations of Ag and Fe ions in the suspension were measured by ICP and equaled to 0.070 and 0.010 mmol/g, respectively.

Disk diffusion assay

To screen the antimicrobial activity of the NP, initially, disk diffusion test was used. Briefly, the tested microorganisms were cultured on proper media. Then, the microorganism strains were suspended in 5 mL of normal sterile saline solution and mixed with vortex thoroughly to obtain a homogeneous suspension. Optical density (OD) of the prepared suspensions was adjusted to reach a turbidity of 0.5 McFarland standards. A swab of sterile cotton, which was moistened by the inoculum suspension, was rubbed on a plate with 90 mm diameter filled with Müller-Hinton agar and supplemented by 2% glucose (for organism nutrition and growth) and 0.5 µg/mL methylene blue (to enhance definition of the zone edge). The plates were dried for 3–10 min. Then, the patterns of antibacterial susceptibility of the NP were determined by soaking the blank disks in NP solutions and drying the Petri dishes in air. After that, the disks were dispensed onto the inoculated plates, the plates were incubated at 37°C for 24 h, and the inhibition zones around the disks were read.

L. major cytotoxicity assay: parasite culture

MRHO/IR/75/ER *L. major* promastigotes was cultured in the RPMI-1640 medium including L-glutamine, 10%–20% fetal calf serum (FCS) and antibiotics at 24°C for 3 days. Each time, 3×10^6 promastigotes were transferred to 4 mL of the enriched RPMI-1640 medium.

L. major promastigotes were moved to 96-well plates, treated with various NP concentrations and tracked using a light microscope. After 24 h exposure, 25 µL of 5 mg/mL 3-(4,5-dimethylthiazol-2-yl)-2,5-diphenyltetrazolium bromide (MTT) was added to each well, and the plate was incubated for 4 h at 24°C–25°C. The well supernatants were completely removed without disturbing the cell sediments. Then, each well received 100 µL of dimethyl sulfoxide (DMSO). The microplate was shaken for 15 min. After that, the absorbance of the well contents was recorded at 570 nm using a microplate reader. Cell viability was calculated using the following formula: viable cells (%) = (AT − AB)/(AC − AB) × 100, where AC, AT and AB are the absorbances of the untreated (negative control), treated and blank samples, respectively. Viability of the treated and untreated promastigotes was concerned through measuring MTT conversion to its reduced form, which is a measure of cell viability. If the amount of MTT declined, then the toxicity of the NP for promastigotes was declared.

Cell morphology study

The impact of the NP on bacterial cell morphology was evaluated using atomic force microscopy (AFM; Vecco,

San Jose, CA, USA). MIC_{50} dosage of the NP was used to treat fresh bacterial cultures (OD 0.2) for 3 h. Then, the cells were washed with a saline phosphate buffer (pH 7), and 2.5% glutaraldehyde was added to them.[11] A drop of the diluted cell suspension was inserted on a cover slip and vacuum dried prior to AFM studies.

MTT assay

Since Fe_3O_4@PEG–Ag might be toxic to both pathogenic and animal cells, a toxicological assay was conducted on a human cell line to diagnose any health risks during practical applications of the NP. Adipose-derived mesenchymal stem cells (ADMSCs) were purchased from Stem Cell Laboratory of Shiraz University of Medical Sciences and seeded in a 96 well-plate. A total of 5,000 cells/well were used in 100 mL of Dulbecco's Modified Eagle's Medium (DMEM) that was supplemented with 10% fetal bovine serum (FBS) and incubated at 37°C for 4 h in a 5% CO_2 incubator. After cell cohesion, the supernatant was replaced with an equal volume of fresh medium, and the plate was incubated for 24 h. The well contents were prepared by serial dilution of Fe_3O_4@PEG–Ag (2, 4, 8, 16, 32, 64, 128, 256, 512 and 1,024 µg/mL). The control wells consisted of the culture medium with no NP. All NPs and control samples were put in three plate wells to validate the results statistically. After 24 h of cell incubation with various NP concentrations, including the control group, the growth medium was removed and 100 mL of MTT was added to the wells. Incubation was prolonged for 3 h. Then, the medium was removed, and formazan crystals were dissolved in 100 mL of DMSO for 15 min in the incubator. Absorbance of the well contents was read at 595 nm by an enzyme-linked immunosorbent assay (ELISA; Bio-Rad Laboratories Inc., Hercules, CA, USA) reader. Cell percentage viability was defined according to the following formula: cell viability = $(I_{sample}/I_{control}) \times 100$.

Results and discussion

Morphological study

The morphology of the relatively homogeneous NPs synthesized through coprecipitation was studied using field emission scanning electron microscopy (FESEM; Figure 1). To gain more insight into the morphology, shape and size of the NPs, transmission electron microscopy (TEM) was carried out. TEM microscopy unraveled relatively good dispersity of the NPs featuring 20–25 nm spherical core/shell morphology (Figure 2). In addition, the TEM image revealed immobilization of a 5 nm thick layer of PEG coated on the surface of Fe_3O_4 NPs, which demonstrated the core/shell structure of Fe_3O_4@PEG–Ag.

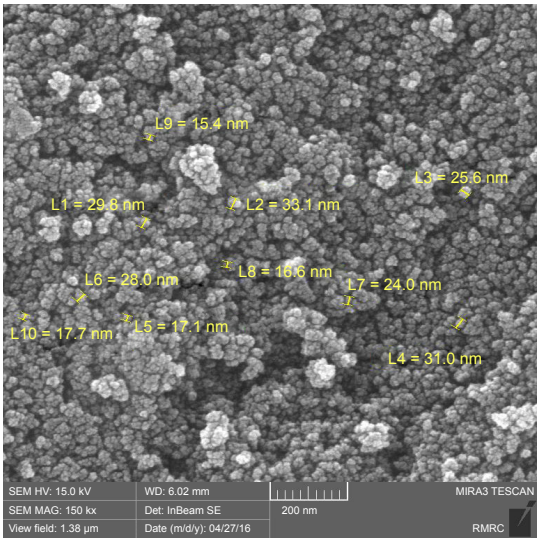

Figure 1 FESEM image of Fe_3O_4@PEG–Ag core/shell nanostructure.
Abbreviations: FESEM, field emission scanning electron microscopy; PEG, poly(ethylene glycol).

In addition to scanning electron microscopy (SEM) imaging, qualitative information about distribution of different chemical elements that are present in the matrix of the NPs was provided by combining SEM with a wavelength-dispersive X-ray (WDX) detector. The representative SEM image and the associated elemental map of Fe_3O_4@PEG–Ag are displayed in Figure 3. As it can be seen in this figure, Ag particles have dispersed well in the composite. Uniformity of the prepared NPs was confirmed by the homogeneous existence of C, O, Fe and Ag throughout the sample based on elemental analysis of the selected area.

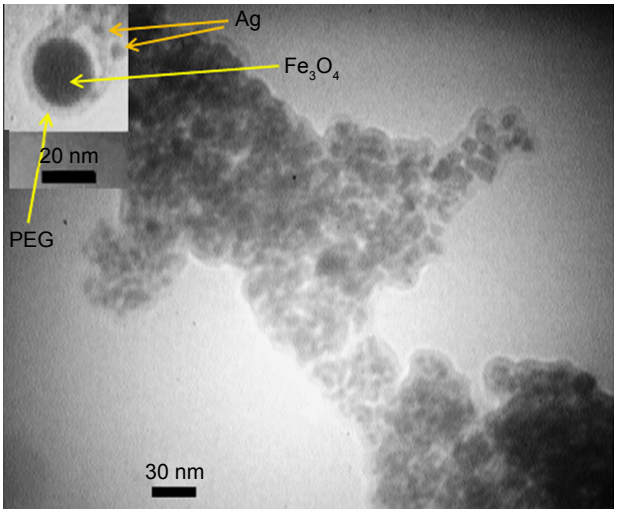

Figure 2 TEM image of Fe_3O_4@PEG–Ag core/shell nanostructure: the electrostatic forces between Fe_3O_4, PEG and Ag are the basis of the nanocomposite formation.
Abbreviations: TEM, transmission electron microscopy; PEG, poly(ethylene glycol).

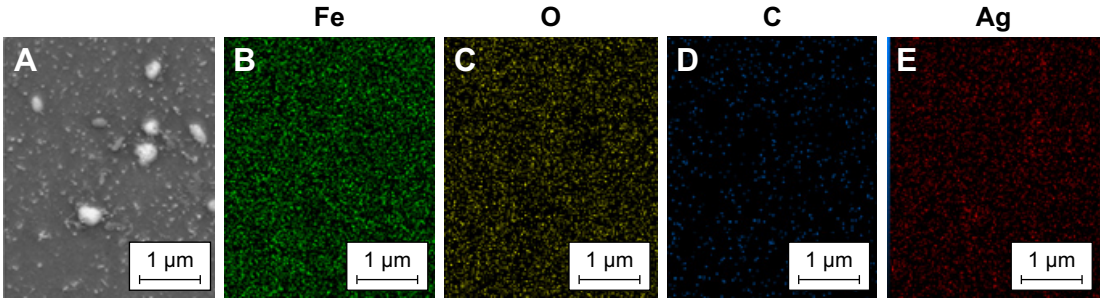

Figure 3 (**A**–**E**) correspond to elemental mapping (WDX) of composite Fe_3O_4@PEG–Ag, Fe, O, C and Ag, respectively.
Abbreviations: WDX, wavelength-dispersive X-ray; PEG, poly(ethylene glycol).

The surface chemical structure of Fe_3O_4@PEG NPs was characterized by Fourier-transform infrared (FT-IR) spectroscopy. The FT-IR spectrum of PEG-coated Fe_3O_4 NPs is illustrated in Figure 4. The presence of magnetite NPs was approved by the appearance of Fe–O bond characteristic absorption at ~563 or 580 cm^{-1}.[30] Furthermore, attachment of PEG on the Fe_3O_4 surface was further verified by observing 2,887 cm^{-1} (C–H asymmetric stretching) and 1,115 cm^{-1} (C–O–C stretching) peaks that are attributed to amorphous PEG.

Energy-dispersive X-ray spectrum (EDS) of the NPs is presented in Figure 5, which includes several signals related to carbon, silver, oxygen and iron. The rise of strong signals in the regions associated with iron and silver declared formation of the nanocomposite of interest. As expected, typical Fe nanocrystals' optical absorption peaks are located at ~1.0 and 7.0 keV because of surface plasmon resonance. Here, higher amounts of C, N and O are observed due to the presence of PEG as the NP's shell.

A vibrating sample magnetometer (VSM) was used to analyze the magnetic properties of Fe_3O_4@PEG–Ag NPs (Figure 6). As depicted in this figure, Fe_3O_4@PEG–Ag can show 26.6 $emu \cdot g^{-1}$ saturation magnetization. This value indicates the adequacy of the NPs' magnetism to facilitate their magnetic separation.

Antimicrobial properties of the nanocomposite

The antibacterial activity of the nanocomposite against *E. coli* and *S. aureus* was evaluated in the agar medium and broth dilution, while its antifungal activity was investigated against *C. albicans*, as one of the pathogenic species, using broth dilution. The results including the inhibition zones of the positive control (tetracycline) are depicted in Figure 7. The solid test displayed the widest diameter of inhibition zone on the bacteria species for the positive control. Comparison of the findings related to the magnetic NPs, ie, Fe_3O_4, Fe_3O_4@PEG and Fe_3O_4@PEG–Ag, distinguished the role of silver NPs loaded on the PEG layer in observation of the NP's antibacterial properties (Table 1). In addition, its superior

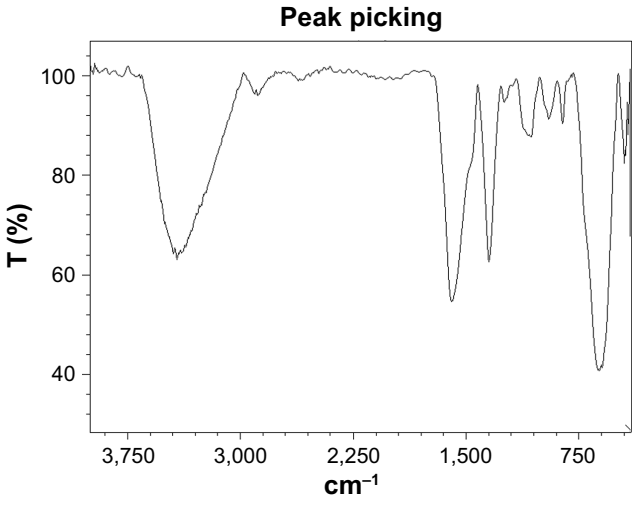

Figure 4 FT-IR spectra of Fe_3O_4@PEG–Ag.
Abbreviations: FT-IR, Fourier-transform infrared; PEG, poly(ethylene glycol); T, transmittance.

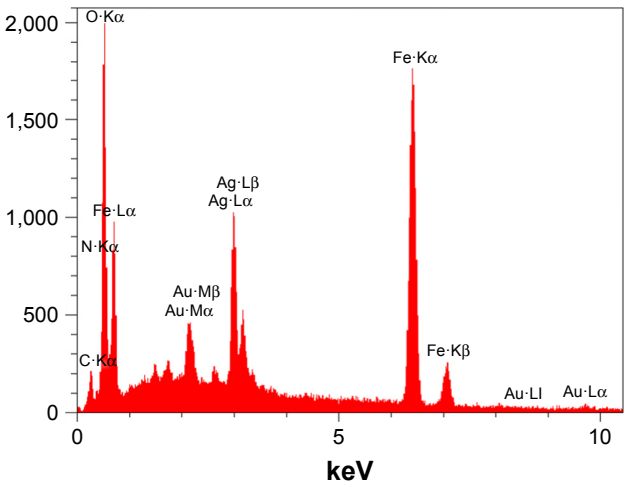

Figure 5 EDS of Fe_3O_4@PEG–Ag.
Abbreviations: EDS, energy-dispersive X-ray spectrum; PEG, poly(ethylene glycol).

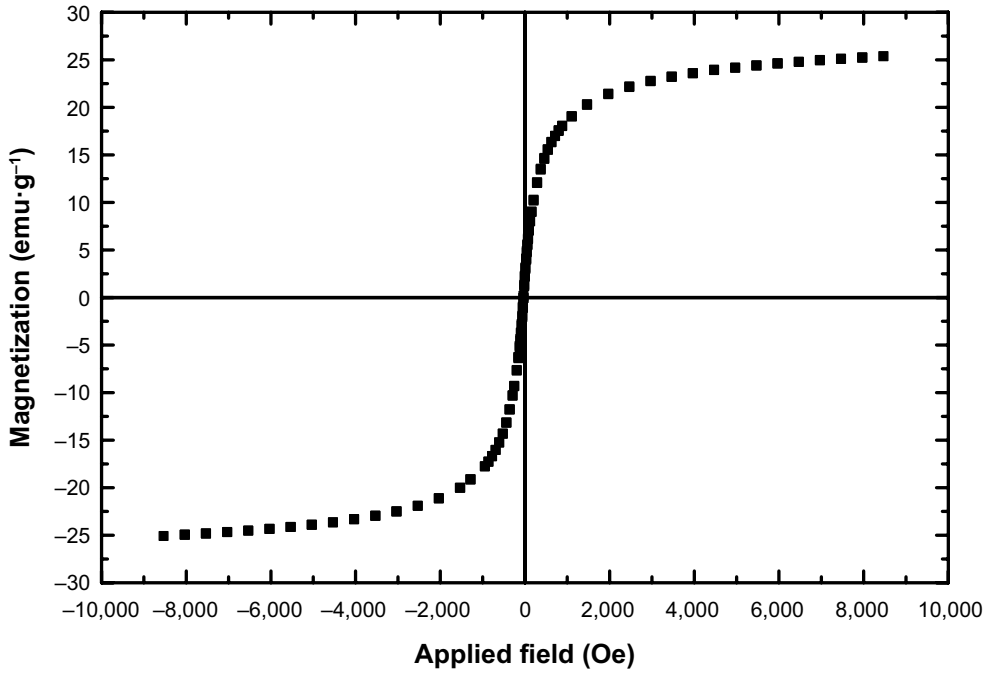

Figure 6 VSM image of Fe_3O_4@PEG–Ag.
Abbreviations: VSM, vibrating sample magnetometer; PEG, poly(ethylene glycol).

antibacterial activities against *S. aureus* in comparison with *E. coli*, MIC, MBC and MFC are summarized in Table 2.

MTT assay

Performing MTT assay showed that exposing the cells to the NP for 24 h can provide the concentration-dependent cytotoxicity (Figure 8). At 2, 4 and 8 µg/mL NP concentration, the viability of the cells after 24 h of incubation was 98.5%, 89% and 100%, respectively. Elevating NP concentration (16, 32, 64, 128, 256, 512 and 1,024 µg/mL) resulted in reduced percentage of cell viability from 100% to ~50% after 24 h.

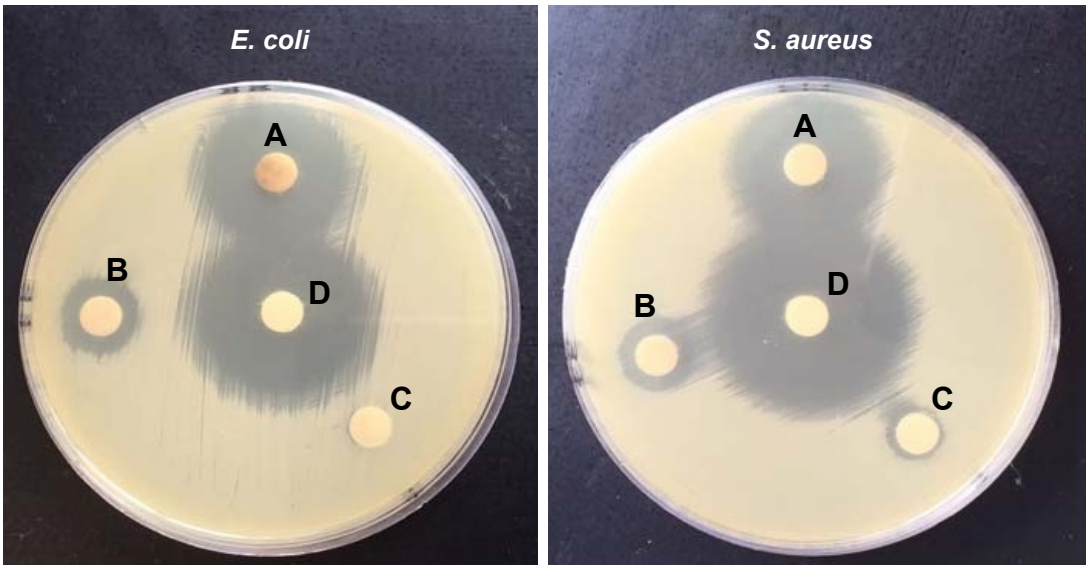

Figure 7 Antibacterial activity of Fe_3O_4@PEG–Ag nanostructures against human pathogens: (**A**) Fe_3O_4@PEG–Ag, (**B**) Fe_3O_4 NPs, (**C**) Fe_3O_4@PEG and (**D**) positive control (tetracycline).
Abbreviations: PEG, poly(ethylene glycol); NP, nanoparticle; *E. coli*, *Escherichia coli*; *S. aureus*, *Staphylococcus aureus*.

Table 1 Antibacterial activities of nanocomposites (diameter of inhibition zone [mm])

Pathogenic strains	Zone of inhibition			
	Fe_3O_4@PEG–Ag	Fe_3O_4@PEG	Tetracycline	Fe_3O_4
E. coli	27 ± 0.2	2.5 ± 0.2	29 ± 0.5	10 ± 0.7
S. aureus	30 ± 0.2	9 ± 0.9	33.5 ± 0.3	11 ± 0.2

Note: Values are expressed as mean ± SD.
Abbreviations: PEG, poly(ethylene glycol); *E. coli*, *Escherichia coli*; *S. aureus*, *Staphylococcus aureus*.

L. major cytotoxicity assays

L. major promastigotes distributed among the plate wells were treated with various NP concentrations and analyzed using a light microscope (Figure 9). After 24 h of exposure to NPs, 25 µL of 5 mg/mL MTT was added to each well. Then, the plate was incubated at 24°C–25°C for 4 h. In the next step, supernatants of the wells were removed completely without perturbing the precipitated cells, and 100 µL of DMSO was added to each well. The microplate was shaken for 15 min, and the absorbance of the well solutions was recorded at 570 nm by a microplate reader. Cell viability was determined using the following formula:

$$\text{Viable cells (\%)} = (AT - AB)/(AC - AB) \times 100$$

where AC, AT and AB correspond to the absorbances of the untreated (negative control) samples, treated samples and blank wells, respectively. Viability of treated and untreated promastigotes was explored by considering MTT conversion to its reduced form. In this way, lower cell viability, ie, declined MTT concentration, is indicative of NP toxicity to the promastigotes.

AFM analysis of the bacterial cells showed that NPs affect the microorganisms' cell walls, and shrinkage morphology of their cells has been shown in Figure 10.

Table 2 MIC (µg/mL), MBC (µg/mL) and MFC (µg/mL) of Fe_3O_4@PEG–Ag for various microorganisms

Strains	MBC/MFC (µg/mL)	MIC (µg/mL)
E. coli	32	16
S. aureus	32	16
C. albicans	16	8

Abbreviations: MBC, minimum bactericidal concentration; MFC, minimum fungicidal concentration; PEG, poly(ethylene glycol); *E. coli*, *Escherichia coli*; *S. aureus*, *Staphylococcus aureus*; *C. albicans*, *Candida albicans*; MIC, minimum inhibitory concentration.

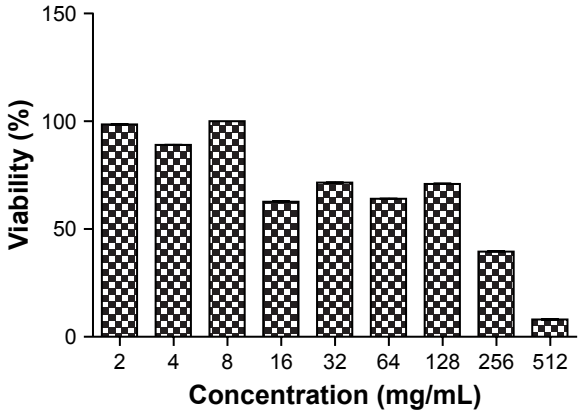

Figure 8 Cell viability was measured by MTT assay.
Abbreviation: MTT, 3-(4,5-dimethylthiazol-2-yl)-2,5-diphenyltetrazolium bromide.

Conclusion

In this study, Fe_3O_4@PEG–Ag NPs were synthesized by relying on electrostatic forces and a reducing agent. The structural properties of the NPs were determined through FT-IR, FESEM–EDS, VSM, ICP-MS and TEM techniques. Furthermore, the antimicrobial activity of the NPs was investigated by exposing the particles to several pathogenic microorganisms including *S. aureus*, *E. coli* and *C. albicans* in the framework of broth microdilution method. In addition, the toxicity of the NPs for the animal cell line was evaluated by the MTT assay. The findings revealed that Fe_3O_4@PEG–Ag nanocomposite can be one of the promising antimicrobial alternatives with an insignificant toxicity. Moreover, this nanostructure can be applied as a smart drug delivery system with the help of an external magnetic field or can be used as

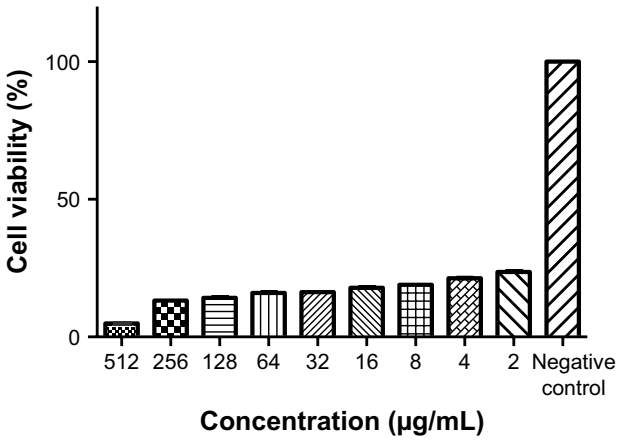

Figure 9 Cell viability was measured by MTT assay.
Notes: Data are shown as mean ± SD with n = 3. $P < 0.0001$ compared with the negative control.
Abbreviation: MTT, 3-(4,5-dimethylthiazol-2-yl)-2,5-diphenyltetrazolium bromide.

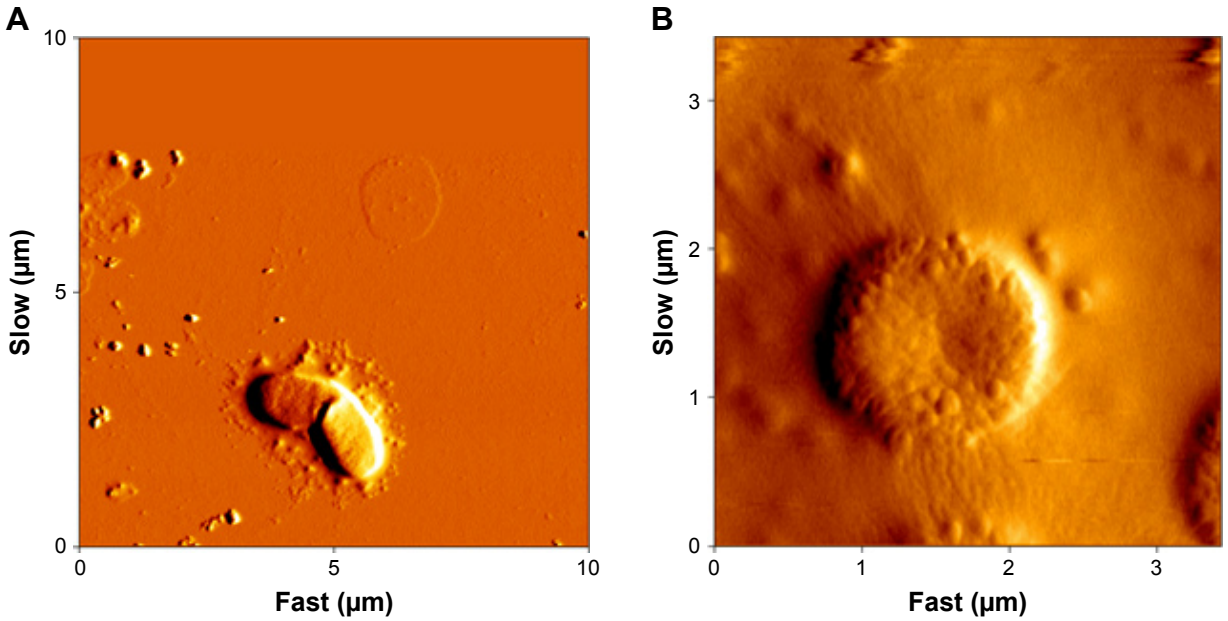

Figure 10 AFM images of Fe_3O_4@PEG–Ag-treated bacterial cells.
Note: (**A**) *E. coli* and (**B**) *S. aureus.*
Abbreviations: AFM, atomic force microscopy; PEG, poly(ethylene glycol); *E. coli*, *Escherichia coli*; *S. aureus*, *Staphylococcus aureus*.

a powerful antibiotic agent along with other antibiotics that can form a shell on its structure.

Acknowledgment

We are grateful to Payame Noor University (PNU) and Shiraz University of Medical Sciences for financial support.

Disclosure

The authors report no conflicts of interest in this work.

References

1. Zhang Z, Yue X, Wei D, et al. DMSO-based PbI_2 precursor with $PbCl_2$ additive for highly efficient perovskite solar cells fabricated at low temperature. *RSC Adv*. 2015;5(127):104606–104611.
2. Ye E, Regulacio MD, Bharathi MS, et al. An experimental and theoretical investigation of the anisotropic branching in gold nanocrosses. *Nanoscale*. 2016;8(1):543–552.
3. Hidron AI, Edwards JR, Patel J, et al. Antimicrobial-resistant pathogens associated with healthcare-associated infections: annual summary of data reported to the National Healthcare Safety Network at the Centers for Disease Control and Prevention, 2006–2007. *Infect Control Hosp Epidemiol*. 2008;29(11):996–1011.
4. Mayrhofer S, Paulsen P, Smulders FJ, Hilbert F. Antimicrobial resistance profile of five major food-borne pathogens isolated from beef, pork and poultry. *Int J Food Microbiol*. 2004;97(1):23–29.
5. Sundar S. Drug resistance in Indian visceral leishmaniasis. *Trop Med Int Health*. 2001;6(11):849–854.
6. Hadighi R, Mohebali M, Boucher P, Hajjaran H, Khamesipour A, Ouellette M. Unresponsiveness to Glucantime treatment in Iranian cutaneous leishmaniasis due to drug-resistant Leishmania tropica parasites. *PLoS Med*. 2006;3(5):e162.
7. Veisi H, Hemmati S, Shirvani H, Veisi H. Green synthesis and characterization of monodispersed silver nanoparticles obtained using oak fruit bark extract and their antibacterial activity. *Appl Organomet Chem*. 2016;30(6):387–391.
8. Veisi H, Faraji AR, Hemmati S, Gil A. Green synthesis of palladium nanoparticles using *Pistacia atlantica* kurdica gum and their catalytic performance in Mizoroki–Heck and Suzuki–Miyaura coupling reactions in aqueous solutions. *Appl Organomet Chem*. 2015;29(8):517–523.
9. Veisi H, Ghorbani-Vaghei R, Hemmati S, Aliani MH, Ozturk T. Green and effective route for the synthesis of monodispersed palladium nanoparticles using herbal tea extract (*Stachys lavandulifolia*) as reductant, stabilizer and capping agent, and their application as homogeneous and reusable catalyst in Suzuki coupling reactions in water. *Appl Organomet Chem*. 2015;29(1):26–32.
10. Veisi H, Rashtiani A, Barjasteh V. Biosynthesis of palladium nanoparticles using *Rosa canina* fruit extract and their use as a heterogeneous and recyclable catalyst for Suzuki–Miyaura coupling reactions in water. *Appl Organomet Chem*. 2016;30(4):231–235.
11. Keihan AH, Veisi H, Veasi H. Green synthesis and characterization of spherical copper nanoparticles as organometallic antibacterial agent. *Appl Organomet Chem*. 2017;31(7):e3642.
12. Keihan AH, Veisi H, Biabri PM. Facile synthesis of PEG-coated magnetite (Fe3O4) and embedment of gold nanoparticle as a nontoxic antimicrobial agent. *Appl Organomet Chem*. 2017;31(12):e3873.
13. Veisi H, Nasrabadi NH, Mohammadi P. Biosynthesis of palladium nanoparticles as a heterogeneous and reusable nanocatalyst for reduction of nitroarenes and Suzuki coupling reactions. *Appl Organomet Chem*. 2016;30(11):890–896.
14. Pirhayati M, Veisi H, Kakanejadifard A. Palladium stabilized by 3, 4-dihydroxypyridine-functionalized magnetic Fe3O4 nanoparticles as a reusable and efficient heterogeneous catalyst for Suzuki reactions. *RSC Adv*. 2016;6(32):27252–27259.
15. Veisi H, Sedrpoushan A, Maleki B, Hekmati M, Heidari M, Hemmati S. Palladium immobilized on amidoxime-functionalized magnetic Fe3O4 nanoparticles: a highly stable and efficient magnetically recoverable nanocatalyst for sonogashira coupling reaction. *Appl Organomet Chem*. 2015;29(12):834–839.

16. Veisi H, Gholami J, Ueda H, Mohammadi P, Noroozi M. Magnetically palladium catalyst stabilized by diaminoglyoxime-functionalized magnetic Fe3O4 nanoparticles as active and reusable catalyst for Suzuki coupling reactions. *J Mol Catal A Chem*. 2015;396:216–223.
17. Veisi H, Sedrpoushan A, Hemmati S. Palladium supported on diaminoglyoxime-functionalized Fe3O4 nanoparticles as a magnetically separable nanocatalyst in Heck coupling reaction. *Appl Organomet Chem*. 2015;29(12):825–828.
18. Khakiani BA, Pourshamsian K, Veisi H. A highly stable and efficient magnetically recoverable and reusable Pd nanocatalyst in aqueous media heterogeneously catalysed Suzuki C–C cross-coupling reactions. *Appl Organomet Chem*. 2015;5(29):259–265.
19. Ma J, Zhang J, Xiong Z, Yonga Y, Zhao XS. Preparation, characterization and antibacterial properties of silver-modified graphene oxide. *J Mater Chem*. 2011;21(10):3350–3352.
20. Liong M, France B, Bradley KA, Zink JI. Antimicrobial activity of silver nanocrystals encapsulated in mesoporous silica nanoparticles. *Adv Mater Deerfield*. 2009;21(17):1684–1689.
21. Shi Q, Vitchuli N, Nowak J, et al. One-step synthesis of silver nanoparticle-filled nylon 6 nanofibers and their antibacterial properties. *J Mater Chem*. 2011;21(28):10330–10335.
22. Xue W, Huang D, Zeng G, et al. Nanoscale zero-valent iron coated with rhamnolipid as an effective stabilizer for immobilization of Cd and Pb in river sediments. *J Hazard Mater*. 2018;341:381–389.
23. Huang D, Xue W, Zeng G, et al. Immobilization of Cd in river sediments by sodium alginate modified nanoscale zero-valent iron: impact on enzyme activities and microbial community diversity. *Water Res*. 2016;106:15–25.
24. Gong X, Huang D, Liu Y, et al. Stabilized nanoscale zerovalent iron mediated cadmium accumulation and oxidative damage of Boehmeria nivea (L.) Gaudich cultivated in cadmium contaminated sediments. *Environ Sci Technol*. 2017;51(19):11308–11316.
25. Mathew TV, Kuriakose S. Studies on the antimicrobial properties of colloidal silver nanoparticles stabilized by bovine serum albumin. *Colloids Surf B Biointerfaces*. 2013;101:14–18.
26. Chatterjee AK, Sarkar RK, Chattopadhyay AP, Aich P, Chakraborty R, Basu T. A simple robust method for synthesis of metallic copper nanoparticles of high antibacterial potency against *E. coli*. *Nanotechnology*. 2012;23(8):085103.
27. Jayaprakash N, Vijaya JJ, Kaviyarasu K, et al. Green synthesis of Ag nanoparticles using Tamarind fruit extract for the antibacterial studies. *J Photochem Photobiol B*. 2017;169:178–185.
28. Kaufman CL, Williams M, Ryle LM, Smith TL, Tanner M, Ho C. Superparamagnetic iron oxide particles transactivator protein-fluorescein isothiocyanate particle labeling for in vivo magnetic resonance imaging detection of cell migration: uptake and durability. *Transplantation*. 2003;76(7):1043–1046.
29. Mondini S, Cenedese S, Marinoni G, et al. One-step synthesis and functionalization of hydroxyl-decorated magnetite nanoparticles. *J Colloid Interface Sci*. 2008;322(1):173–179.
30. D'souza AJM, Schowen RL, Topp EM. Polyvinylpyrrolidone–drug conjugate: synthesis and release mechanism. *J Control Release*. 2004;94(1):91–100.
31. Edmond MB, Wallace SE, McClish DK, Pfaller MA, Jones RN, Wenzel RP. Nosocomial bloodstream infections in United States hospitals: a three-year analysis. *Clin Infect Dis*. 1999;29(2):239–244.
32. Kaviyarasu K, Kanimozhi K, Matinise N, et al. Antiproliferative effects on human lung cell lines A549 activity of cadmium selenide nanoparticles extracted from cytotoxic effects: investigation of bio-electronic application. *Mater Sci Eng C*. 2017;76:1012–1025.
33. Kaviyarasu K, Geetha N, Kanimozhi K, et al. In vitro cytotoxicity effect and antibacterial performance of human lung epithelial cells A549 activity of zinc oxide doped TiO2 nanocrystals: investigation of bio-medical application by chemical method. *Mater Sci Eng C*. 2017;74:325–333.
34. Magdalane CM, Kaviyarasu K, Vijaya JJ, Siddhardha B, Jeyaraj B. Photocatalytic activity of binary metal oxide nanocomposites of CeO2/CdO nanospheres: investigation of optical and antimicrobial activity. *J Photochem Photobiol B*. 2016;163:77–86.
35. Ezhilarasi AA, Vijaya JJ, Kaviyarasu K, Maaza M, Ayeshamariam A, Kennedy LJ. Green synthesis of NiO nanoparticles using *Moringa oleifera* extract and their biomedical applications: cytotoxicity effect of nanoparticles against HT-29 cancer cells. *J Photochem Photobiol B*. 2016;164:352–360.
36. Kaviyarasu K, Maria Magdalane C, Kanimozhi K, et al. Elucidation of photocatalysis, photoluminescence and antibacterial studies of ZnO thin films by spin coating method. *J Photochem Photobiol B*. 2017;173:466–475.
37. Wayne P. Clinical and Laboratory Standards Institute (CLSI) Method for Dilution Antimicrobial Susceptibility Tests for Bacteria That Grow Aerobically. Approved standard–8th ed. Wayne, PA: CLSI; 2009. CLSI document M07-A8.